Egypt. J. Chem. **Vol. 67**, No. 12 pp. 307 - 317 (2024)

Egyptian Journal of Chemistry

http://ejchem.journals.ekb.eg/

Hematoporphyrin-Gold Nanocomposite as a Smart Generation of Photopesticides to Control Cotton Leafworm Stages, *SpodopteraLittoralis*

Shaimaa M. Salama,[1*] Al-sayed A. Al-Sherbini,[2] Gamal El-Ghannam,[2] Ahmed I. Imam,[1] Wael M. Darwish,[3]

[1]*Department of Plant Protection, Desert Research Center, Mataria, Cairo, 11753, Egypt*

[2] *Department of Measurements, Photochemistry and Agriculture Applications, National Institute of Laser Enhanced Science (NILES), Cairo University, Giza 3725005, Egypt*

[3]*Department of Polymers and Pigments, National Research Centre, Elbohouth Street, Dokki 12622 Giza, Egypt*

Abstract

As a global commodity, cotton plays a major role in the economic and social development of emerging economies and newly industrialized countries. Egyptian cotton occupies a unique and important place in the world market because of its high quality and long staple fiber. Unfortunately, the Egyptian cotton plant has been attacked by *Spodopteralittoralis*leading to huge economic losses. Excessive and uncontrolled use of chemical insecticides resulted in food contamination as well as environmental, agricultural, and aquatic pollution. Nanotechnology opened new avenues for manufacture of more environmentally safe pesticides. Photosensitizers can also contribute to produce cost-effective and ecofriendly pesticides, photopesticides. In this study, we prepared a hematoporphyrin-gold (HP-AuNPs) nanocomposite as a model for smart generation of photopesticides processing high photodynamic cytotoxic actions. The prepared Photopesticides was characterized by UV-VIS spectroscopy, FTIR, and transmission electron microscopy (TEM). The prepared composite exhibited no appreciable toxicity to *S. littoralis* without exposure to light. The prepared nanocomposite exertedhigh phototoxicity against the 2nd instar larvae of the Egyptian cotton leafworm in a concentration-dependent manner (LC_{50} = 0.9 ppm of gold). The performed biochemical analysis of the tested groups revealed that dipping of the second larval instar of *S. littoralis* in aqueous solution of (HP-AuNPs) nanocomposite (LC_{50}) followed by light exposure (halogen lamb 500 W, 4h) resulted in a remarkable incitement of α- and β-esterase activities, alkaline phosphatase, total protein, total carbohydrate, acetyle choline esterase and mixed function oxidase activity.

***Keywords*:** Cotton leaf worm; smart photopesticides, porphyrins; gold nanoparticles

1. Introduction

World cotton production is projected to grow at 1.6% per production is projected to grow at 1.6% per year, increasing from 126.5 million bales in 2022/23 to around 141.3 million bales in 2031/32 [1]. Egypt's cotton production has been growing for the past few decades and is ranked as one of the best cotton products in the world because of its high quality, long staple fiber [2]. In the 1970's, raw cotton production accounted for only 5.4% of the country's total gross domestic product [3]. The crop constitutes 46.2% of the country's total exports and is equivalent to 75.6 % of the country's total agricultural exports [4]. Spodoptera littoralis is one of the most serious agricultural pests and responsible for significant yield losses not only in Egypt but in many regions of the

*Corresponding author e-mail: shaimaabduallah1981@gmail.com.; (Shaimaa M. Salama).
EJCHEM use only: Received date 11 September 2024; revised date 09 October 2024; accepted date 12 October 2024
DOI: 10.21608/EJCHEM.2024.320236.10413

world's well. Cotton is infested during the period between May-July following migration from previous host plant clover Trifolium alexandrinum [5,6]. Losses from the Egyptian Cotton Leafworm are estimated by millions of Egyptian pounds per year [3]. The traditional insecticides formulations dedicated for control programs have negative impacts on environment and public health [7]. Hence, efforts should be taken to reduce waste, production costs, and environmental pollutionfrom one hand and to extend the duration of pesticide activity from the other. The solar energy, in the presence of a proper photoreceptor, was applied for effective control of the pollution of several types of insects. This reduces the environmental impact and minimizes risk for plants, animal and human ecosystem. Porphyrins (Pors) and phthalocyanines (Pcs) are the most widely applied photosensitizers (PSs) in many biological applications such as photodynamic therapy (PDT) of cancer [8]. Compared to the conventional insecticides, these photosensitizers are highly favored because of broad absorption spectrum, biocompatibility, cost-effective production, and photo- degradability [9]. The photosensitization is a photophysical process involves absorption of the light by a proper localized photosensitizer (PS) followed by a photophysical reaction with the molecular oxygen (O_2) present nearby producing reactive oxygen species of high cytotoxicity [10]. Nanoparticles exhibit high biological activity than other forms of material due to their small size and huge surface area. When photosenitizers are applied as solution, they suffer from rapid leakage from the biological environment where they should do their function. At this point, the use of nanoparticles such as gold nanoparticles as carriers for the photosensitizers (PS) affords stability in the biological medium and ability to load high amounts of the PS. The most important advantage of loading the PS at the surface of nanoparticles is the enhanced penetration of the nanoparticles to the targeted cells and tissues via enhanced permeability and retention (EPR) phenomenon [11]. Several studies revealed the biocompatibility of gold nanoparticles (AuNPs) [12,13]. In this work, (HP-AuNPs) nanocomposite was prepared, characterized and evaluated as potential photopesticide. The prepared nanocomposite was bio-assayed against both egg and 2nd instar larval stages of *S. littoralis.*

2. Experimental:

2.1. Materials and chemical characterization

Chloroauric acid ($HAuCl_4.4H_2O$, 99.99%) was purchased from Merck, Germany. Hematoporphyrin (HP, CAS Number 14459-29-1) was a product of Puress (Logan, Utah). IUPAC Name of HP: 3-[18-(2-carboxyethyl)-8,13-bis(1-hydroxyethyl)-3,7,12,17-tetramethyl-22,23-dihydroporphyrin-2-yl]propanoic acid. Glycerine was a product of (puress, BDH). Other solvents were of analytical grade and used as received. UV-visible absorbance spectra was measured using Jenway double beam spectrophotometer and the samples were placed in 1 cm UV-quartz and the absorption was recorded within the appropriate scan range from 200 to 900 nm. FTIR spectra were recorded on an infrared spectrometer (type Jasco FT/IR-430, Japan) using the KBr disc technique. Transmission electron microscopy (TEM) were used to determine the shape and sizes of the prepared samples and illustrate the embedding of gold nanoparticles in the dye were carried out using JEOL (JEM-1400 TEM). The samples were analyzed for gold content (ppm Au) by ICP-OES. The cotton leaf warm stages were exposed to artificial light of halogen lamp of 500 W/m^2in transparent cages surrounding by water bath to keep the optimum temperature.

2.2. Synthesis of hematoporphyrin-gold (HP-AuNPs) nanocomposite

Hematoporphyrine-coated gold (HP-Au NPs) nancompsoite, was prepared by pyrolysis method. About 10 mL of $5x10^{-1}$ mol of ($HAuCl_4$) was added drop wise to 100 mL of glycrine containing 60 mg of hematoporphyrin at 200 °C. Heating continued for another 5 min. After that, the solution was removed from the heater and stirred for further 15 min.The final color observed was winered. The product was isolated via centrifugation (10000 rpm, 10 min). The solid was redispersed in DW followed by centrifugation. This process was trice repeated and the final pure product was redispersed in DW for further use.

2.3. Toxicological studies

2.3.1. Insect colony and determination of LC_{50}

A laboratory strain of the cotton leafworm, *S. littoralis*, was kindly obtained from the Central Agricultural Pesticide Laboratory. The laboratory culture wasestablishedat 25±2 °C and 65±5% R.H. in the insectariums of Plant Protection department, Desert Research center according to the method described by El-Defraw *et al.* [14]. An aqueous stock solution of the tested photosensitizer, hematoporphyrin-gold (HP-AuNPs), was prepared at gold concentration of (100 ppm). Solutions of different gold concentrations (0-20 ppm) were

prepared via dilution with deionized water. the experimental bioassay was carried out by dipping technique. To evaluate LC_{50} of the photosensitizer the castor-bean leaves were dipped for 60 seconds in solutions of different concentrations of the photosensitizer. The treated leaves were then left for drying at room temperature before being offered for all night to larvae. Subsequently, the larvae were exposed to artificial light (500 W) for 4 h then feeding on untreated leaf castor bean for 5 days. At the end of treatment, the larvae were starved for 4 h and kept at -20 °C for biochemical analyses. To check the pesticidal efficacy of the prepared photosensitizer under darkness conditions, comparable treatments had been carried out without exposure to any source of light. The daily larval death was determined every 24 h till the 5th day post treatments. The total larval death percentages (observed values) were calculated and corrected using Abbott's formula [15]. Finally, the LC_{50} values of the photosensitizer was estimated according to [16].

2.3.2. Biochemical assay

This experiment aimed to determine the physiological disorders resulting from the treatment of *S. littoralis* with the photosensitizer at LC_{50}.

(i) Preparation of insects for analyses:

The treated larvae of the cotton leafworm (previously kept at -20 °C) were homogenized by Teflon tissue homogenizer (ST – 2 Mechanic-Preczyina , Poland) in distilled water (10 larvae/ml). The homogenates were centrifuged at 8000 r.p.m. for 15 min at 4 °C in a refrigerated centrifuge . The deposits were discarded and the supernatants were kept at -20 °C till use for biochemical assays. Double beam ultraviolet / visible spectrophotometer (spectronic 1201 , Milton Roy Co. ,USA) was used to measure absorbance of colored substances or metabolic compounds.

(ii) Alpha esterases (α-esterases) and beta esterases (β-esterases)* and (*acetylcholinesterase) activity:

These enzymes were determined according to Van Asperen (I962) using α-naphthyl acetate or β-naphthyl acetate as substrates, respectively. AchE (acetylcholinesterase) activity was measured according to the method described by Simpson *et.al.* [17], using acetylcholine bromide (AchBr) as substrate.

(iii) Mixed function oxidase activity:

P-nitroanisole O-demethylation was assayed to determine the mixed function oxidase activity according to the method of Hansen and Hodgson [18] with slight modification.

(iv) Phosphatases activities:

Acid and alkaline phosphatases were determined according to the method described by Powell and Smith [19].

(v) Total carbohydrates:

Total carbohydrates were estimated in acid extract of larval tissues by the phenol-sulphuric acid reaction of Dubois *et al.*[20]. Total carbohydrates were extracted and prepared for assay according to Crompton and Birt [21].

(vi) Total proteins:

Total proteins were determined by the method of Bradford [22].

2.4. Histological studies

Histological assessment ~~were~~ had been carried out on the 2nd instar larvae of *S. littoralis* by dipping technique. Where, larvae got dipped in the LC_{50} concentration of the photosensitizer solution got subjected to 4 h exposure period to 500 W halogen lamp. After the death of larvae, they were quickly fixed in 2.5% glutaraldehyde in 0.1M chilled phosphate buffered (pH7.3) for 24 h. Subsequently, the samples were treated with osmium tetroxide, dehydrated in different alcohols and embedded in an epoxy resin. Tissue samples were sliced into thin sections of ~600µm thickness using Leica Ultracut UCT ultramicrotome. The sections were finally stained with tolodin blue (1X) and examined by camera Lica ICC50HD as described by Bozzola and Russell [23]. For TEM histological investigations, the fixed samples were sliced to ultra thin sectiones (~ 75-90 µm) and stained with uranyl acetate and lead citrate. TEM images were captured by CCD camera model AMT, optronic camera with 1632*1632pixel formate as side mount configuration. This camera uses a 1394 fire wire boared for acquision.

2.5. Statistical analysis

Using the Ldp line application (http://www.ehabsoft.com/ldpline/), toxicological data, including the LC_{50} of each dye, were calculated using the probit approach [16]. Enzyme measurements were performed in triplicate and the data was reported as the mean ±SE. The data was analysed as one way ANOVA using Proc ANOVA in SAS (Anonymous. 2003), and means were compared using LSD (P= 0.05 level) in the same software.

3. Results and Discussion

The concept of photopesticides has gained recently great momentum as low-cost and eco-friendly alternative to the chemical pesticides. The usage of chemical pesticides usually used in Egypt cotton farming has unfortunate side effects for many non-target organisms such as natural predators and

pollinators. A recent study [24] has revealed that the use of synthetic pesticides led to an average of 60 – 80% reduction in non-target species. These non-target organisms are valuable to agriculture and the environment and their value is largely underestimated [15]. It was found that *Spodoptera littoralis larvae* collected from a cotton field that was heavily sprayed with conventional insecticides showed strong resistance to Organophosphorous and Pyrethroid [25]. The repeating of the use of various insecticides showed strong resistance toward the warm and became not efficient to control the insects [26].

This work aimed at the development of new approaches to the building up of new photopesticides based on nanotechnology. Hematoporphyrin (HP) is a good photoreceptor usualy used to exert several photodynamic cytotoxic actions. However, the poor water solubility of HP limits its use in certain biological applications. Conjugation of HP to the surface of a hydrophilic nanoparticles dipsersed in water, such as AuNPs, lead to formation of water dispersable HP-AuNPs nancomposit (Fig. 1). This conjugation results in a homogeneous distribution of the photrecepetor (HP) on the surface of the nanoparticles and consequently optimize its photobiological actions. In this work, in-situ method was used for production of (HP-AuNPs) nancomposite. This one-pot concept led to facile and cost-effective production of the targeted conjugate as a winered solution.

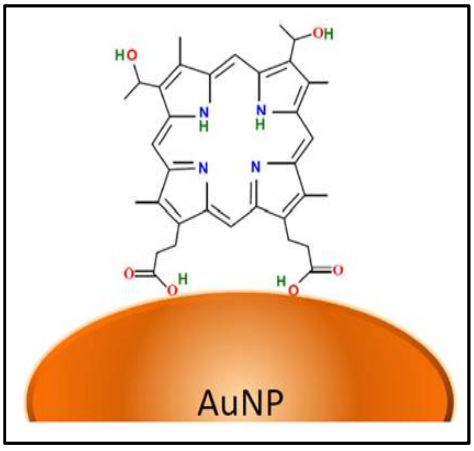

Figure 1: Structure of (HP-AuNPs) nanocomposite.

3.1. Characterization

High-resolution TEM image of (HP-AuNPs) nanocomposite (Fig. 2) shows spherical nanoparticles of size range (13±8 nm) and other shapes of gold nanoparticles such as triangles gold nanoparticles. The nanospheres are nearly monodisperesed and characterized with smooth surface morphology.
It is well known that high-temperature synthesis of gold nanoparticles especially in the presence of organic compounds e.g. phenols or HP leads probably to formation of multi-shaped gold conjugate nanoparticles since the gold nanoparticles are inherently coated by a dense network of the organic molecules [27].

UV-Vis absorption spectra of HPand (HP-AuNPs) nanocomposite are shown in Fig. 2. Free HP exhibited an intense soret B-band at $\lambda_{max.}$=350 nm and other four weak satellite Q-bands at λ_{max} = 505, 538, 567,617 nm [28a]. On the other hand, aqueous solutionof (HP-AuNPs) nanocomposite shows two absorption bands at λmax. =637± 5 nm and 677±5 nm, in addition to an intense band at $\lambda_{max.}$= ~ 350 nm (Fig. 3). These two bands are probably attributed to formation of a stable HP-AuNP nanocomplex accompanied with a crystal growth of the gold nanoparticles to variable sizes and shapes and appearance of red-shifted absorption profile to that well-known of gold nanoparticles (λmax.= ~ 520-550 nm) [28a-b]. Upon assembly of HP at the surface of AuNPs, a new band starts to appear at higher wavelength with λmax~ 637 nm in the absorption spectrum of HP-AuNPs nanocomposite as shown in Fig. 3. The appearance of the new band at 637 nm was accompanied by disappearance of the SPR band of AuNPs at 525 nm. This shift is due to the change in the dielectric constant of the solution [28b]. Another new band that appeared at higher wavelength~677 nm in the absorption spectra of HP-AuNPs nanocomposite is probably attributed to the assembly of nanoparticles. It is known that the apparition of the broad peak at longer wavelengths in the absorption spectrum comes from the coupling of surface plasmon resonance (SPR) of two adjacent gold nanoparticles and it is an indication of the anisotropic optical properties of the AuNPs agglomeration [28b].

FTIR spectra of HP and (HP-AuNPs) nanocomposite are shown in Fig. 4. The characteristic stretching and bending vibrations of HP [29] are also found in the spectra of HP-AuNPnanocomposite and this confirms the successful coating of gold nanoparticles with HP. The broad band (3000-3700 cm^{-1}) can be assigned to the OH groups present in HP molecule. Bands of medium intensity at 2950 and 2895 $^{-1}$ can be assigned to aliphatic –CH bonds in HP molecules. The bands at 1720 cm^{-1} are assigned to the stretching vibration of the carbonyl groups present in HP molecule [30].

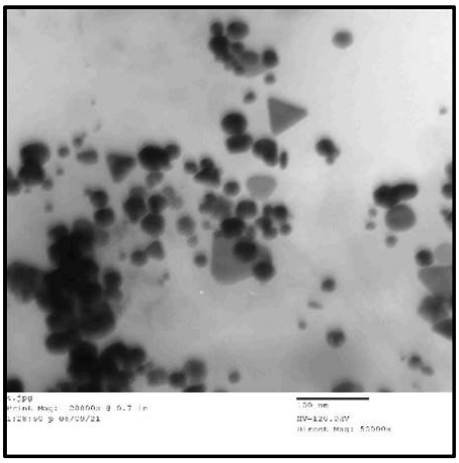

Figure 2: High-resolution TEM micrographs of (HP-AuNPs) nanocomposite.

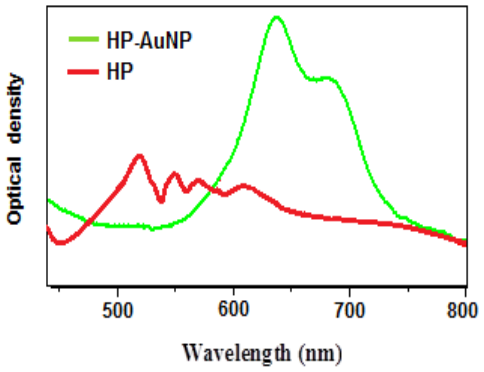

Figure 3: UV-Vis spectra of HP and (HP-AuNPs) nanocomposite in water.

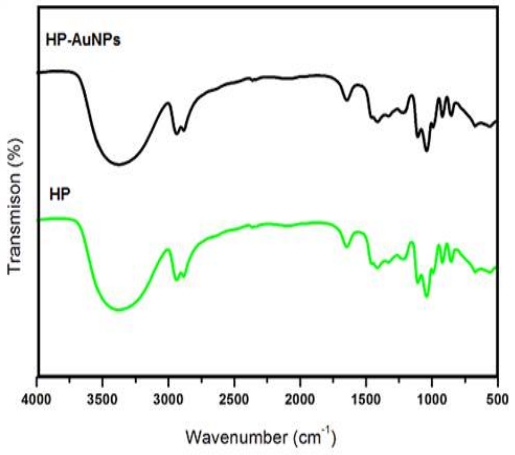

Figure 4: FTIR spectra of HP and (HP-AuNPs) nanocomposite.

3.2. Toxicological studies

The 2nd instar larvae of *S.littoralis* were treated with different concentrations of (HP-AuNPs) nanocomposite followed by keeping in dark or exposure to artificial light (500 W/m^2) at 25 ^{o}C for 2 and 4 h. Subsequently, the percentage of mortality was determined at different time intervals (1-5 days). The results illustrated that no mortality was observed in the absence of light. Treatment followed by 4 h exposure to 500 W artificial light showed concentration-dependant larval death (Fig. 5) that ranged from 21.81% to 95 %. The calculated LC_{50} was 0.9 ppm of gold. The findings support the need for additional research using hematoporphyrin-gold nanocomposites in vivo on insects in order to identify the true prospects of the nanocomposites application in photodynamic therapy.

HP concentration in the bait, the irradiation fluence rate, and the total light dose all affected how long the HP-fed flies survived after being exposed to light that resembled the solar spectrum. 100% mortality was achieved in 1 hour of light exposure for 8 µmol/mL HP in the bait, with a fluence rate of 1220 µE $s^{-1}.m^{-2}$ for *C. capitata* and 2080 µE $s^{-1}.m^{-2}$ for *B. oleae*. Because it had swallowed less HP and/or had darker pigmentation, the latter fly was somewhat less photosensitive than *C. capitata* [31]. The results of the treatment showed dose-dependent mortality, which reached 100% after 6 h of rose bengal therapy and 90.6% after 24 h of chlorpyrifos treatment. The LC_{50} of rose bengal and chlorpyrifos were $4.9x10^{-6}$ and $4.9x10^{-4}$, respectively, six hours after treatments; the LC_{95} were $2.0x10^{-3}$ and $4.0.10^{-3}$., respectively against the early 3rd larval instar of *Culex pipiens* [32].

Various hematoporphyrin-gold nanocomposites were obtained, which contained similar hematoporphyrin concentration (5 µg/ml) and varied concentrations (0.5–5 µg/ml) of gold nanoparticles with a diameter of 15 nm or 45 nm. It appears that the larger particles' capacity to carry more porphyrin molecules into cancerous cells accounts for the superior activity of the nanocomposite with ~45 nm gold particles compared to those with 15 nm gold particles, as evidenced by the experiment results.The results obtained warrant the necessity of further studies with hematoporphyrin-gold nanocomposites in vivo on transplanted tumors of animals which have to define the real perspectives of the nanocomposites application in PDT [33].

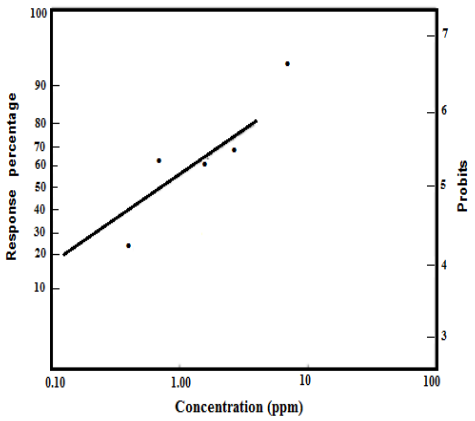

Figure 5: Regression line of mortality study after dipping 2nd instar larvae of *S. littoralis* at 500 W for 4 hours with aqueous solution of (HP-AuNPs) nanocomposite (gold concentration = 0-7 ppm).

3.3. Biochemical study

The performed biochemical analysis of the tested groups revealed that dipping of the second larval instar of *S. littoralis* in aqueous solution of (HP-AuNPs) nanocomposite (LC_{50}) for 4 h followed by light exposure (halogen lamb 500 W) resulted in a remarkable incitement of α- and β-esterase activities, alkaline phosphatase, total protein, total carbohydrate, acetyle choline esterase and mixed function oxidase activity (Tables 1-3).

(i) α- and β-esterase activity

As shown in Table 1, treatment of the second larval instar of *S. littoralis* with LC_{50} of (HP-AuNPs) nanocomposite followed by light resulted in a remarkable incitement of both α- and β-esterase activities. For β-esterase, activity values of 1263.3, 1040 µmole substrated oxidized /min g b.wt for (HP-AuNPs) nanocomposite and the control, respectively. Statistic at P< 0.05 appeared that photoactivated (HP-AuNPs) nanocomposite resulted in a significant increase in β-esterase activity. The activity of β-esterase was increased by 21.5% compared to the control as shown in Table 1 and Fig. 6. For α-esterase, activity values of 632.33,687.33 µ mole substrated reduced /min g b.wt were observed for (HP-AuNPs) nanocomposite and control, respectively. Statistics at P= 0.05 revealed that photoactivated (HP-AuNPs) nanocomposite showed a significant decrease in α-esterase activity. The activity of α-esterase was reduced by 8% compared to the control. A previous study[34] Result indicated that sub-lethal concentrations of sodium copper chlorophyllin and magnesium copper chlorophyllin on field and susceptible strains *Spodoptera littoralis*. The concentration (10-2 M) for both sodium copper chlorophyllin and magnesium copper chlorophyllin was more effective than concentration (10-3 M) on field strains and susceptible strains of Spodoptera littoralis. β-esterase activity showed significant activity increase, and α-esterase showed significant activity reduction in most treatment after estimating them in the total body homogenates on the other hand the acetylcholinesterase activity show lowvarious.

Table 1: Changes in (α- and β- esterase) after treatment of the 2nd instar larval of *S. littoralis* with $LC_{50}$of (HP-AuNPs) nanocomposite (dipping method)

	β-Esterase		α-Esterase	
Sample	Mean ± SE	Change	Mean ± SE	Change
Control	1040±30.6[b]	0	687.3±18.9[c]	0.0
HP@*Au*NPs	1263.3±31.7[a]	21.5	632.33±9.5[d]	-8.0
	F value >0.05		*F value <0.05*	
	P value= 25.65		*P value= 20.15*	
	LSD = 122.43		*LSD =54.7*	

Means with the same letter are not significantly different.

(ii) Phosphatases enzyme activity

As shown in Fig. 6 and Table 2, there was a slight decrease of phosphatase activity change ratio compared to the control treatment.Alcohol and phosphoric acid undergo an esterification process that results in the formation of organophosphates. These substances are widely used in the production of plastics and solvents, as well as being the main ingredients in pesticides, herbicides, and insecticides. The 4th larval instars of *Agrotis ipsilon* larvae in, field experiments were approved to evaluate the effectiveness of certain photosensitizercompounds methylene blue, bromophenol blue and safranin belonging to various chemical groups against *Agrotis ipsilon* larvae in potato cropin El- Giza Governorate in Egypt for the duration of two successive seasons, February 2020 and 2021 underfieldconditions using double values of LC_{50} and LC_{90} of these compounds. On thelight of the median and quarter lethal effects of the three tested photosensitizer compounds, on the total proteins, total lipids, cholinesterase, acid and alkaline phosphatase, the resultsproved that all tested compounds caused decreased in these biochemical contents exceptbromophenol blue treatment slightly increase inacid phosphatase at LC_{25} and methylene blue increased in total lipids [35].

(ii) Acetyl choline activity

As illustrated in Table 2 and Fig. 6, treatment with the photosensitizer resulted in a slight decrease of acetyl choline activity. [36] HpD was investigated as photoinsecticide against 3rd larval instar and adults of a myiatic fly. Third instar larvae and adults from Parasarcophaga argyrostoma (Robineau Desvoidy) (Sarcophagidae: Diptera) were fed baits containing 5xl02, 5x 103, 5x 104, 5x 105, and 5x 106 ppm of HpD photosensitizer. Mortality ratios were recorded at different post treatment sunlight exposure periods. The impact of a single median dose of 5x 104 ppm was studied biochemically, and the results showed that it might destroy defence enzymes like Ach estrase beyond repair. Furthermore, deadly histological alterations were found in the midgut epithelium.

(iii) Mixed Function Oxidase (MFO)

Biochemical analysis revealed that treatment of the second larval instar of *S. littoralis* with LC_{50} of the photosensitizer led to a slight increase of MFO system activity to 68.5, compared to 67.23 µ mole of the control. Substrated oxidized/min/g b.wt for HP@AuNPs and control are shown in Table 2 and Fig. 6. The LC_{50} ofHP@AuNPs phtosensitizer showed a slightly decrease in its activities. Similar increase of MFO was previously reported after treatment of *Spodoptera littoralis* with Chlorophyll in Dye [37].

(vi) Total protein and total carbohydrates

The main metabolites (total proteins, total carbohydrates and total lipids) are major biochemical components necessary for an organism to grow and perform its necessary vital activities. Thus, it may be of interest to study changes in the total protein and total carbohydrate after treatment of the larvae with the prepared nanophotopesticide. As shown in Table 3 andFig. 6, treatment with the prepared photopesticide followed by light exposure resulted in a sharp decrese of both total protein and total carbohydrate relative to control groups. Researchers have looked into the potentially harmful effects of photosensitisers, especially hematoporphyrin (HP). to Oreochromis niloticus, the Nile tilapia. The fish group's adult specimens showed damage to their gills, liver, and kidney tissues after being exposed to HP at lethal concentrations (0.2×10-3 Mol/l) for 96 hours and sublethal concentrations (0.2×10-4 Mol/l) for 12 weeks. Growth indices, RBCs, Ht, Hb, serum total protein, total lipids, and (reduction in muscle total protein and totallipids with an increase in muscle water content) significantly decreased (at $P < 0.01$) in comparison to the control fish group[38].

Table 2: Changes in alkaline phosphatase-esterases (APE), acetyl choline actvity, and MFO after treatment of the 2nd instar larval of *S littoralis* with LC_{50} of (HP-AuNPs) nanocomposite (dipping method)

Sample	APE		acetyl choline		MFO	
	Mean ± SE	Change	Mean ± SE	Change	Mean ± SE	Change
Control	10.8±0.6[a]	-3.1	234.33±12.33[a]	1.4	67.2±1.467[a]	4.9
HP@AuNPs	9.8±0.12[a]	-8.7	196.7±3.8[b]	-16.0	68.6±1.6[a]	1.9
	F value >0.05		F value <0.05		F value <0.05	
	P value= 2.17		P value= 8.50		P value= 0.38	
	LSD= 1.7		LSD= 2.8		LSD= 6.2	

Means with the same letter are not significantly different.

Table 3: Changes in total protein and total carbohydrates after treatment of the 2nd instar larval of *S. littoralis*with LC_{50} of (HP-AuNPs) nanocomposite (dipping method)

	Total Protein		Total Carbohydrate	
Sample	Mean ± SE	Change	Mean ± SE	Change
Control	87.7±1.8[a]	0	16.5±0.76[a]	0.0
HP@AuNPs	58.9±1.6[b]	-32.77	10.7±0.37[b]	-34.9
	F value <0.05		F value <0.05	
	P value= 138.01		P value= 46.12	
	LSD=6.8		LSD= 2.4	

Means with the same letter are not significantly different.

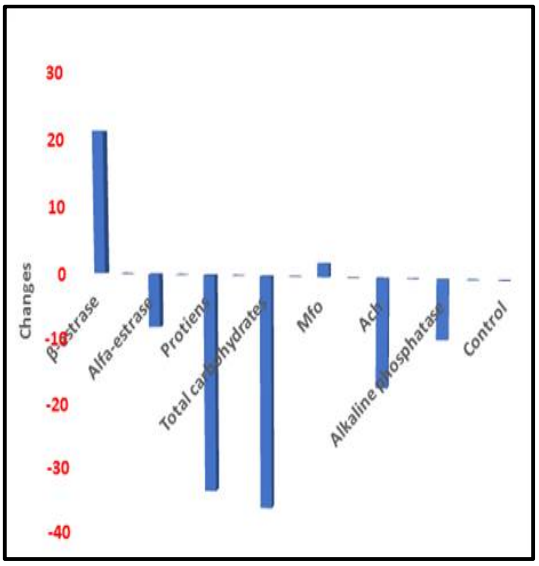

Figure 6: Biochemical analysis after treatment of the 2nd instar larval of *S. littoralis* with LC_{50} of (HP-AuNPs) nanocomposite (dipping method).

4. Histological study

As shown in Fig. 7, the normal midgut of 2nd larval instars of *S. littoralis* consists histologically of the outer sheath of the intestine includes two types of muscles. The outer one is composed of one layer of longitudinal muscles, and the inner one is a layer of circular muscles. The musclosa is followed internally by a thin basement membrane upon which the epithelium rests. The epithelium consists of a layer of epithelial cells, which are elongated and columnar in shape. Each cell contains a dark round nucleus occupying the middle parts of each cell. There are other types of epithelial cells, the regenerative, or the imaginal cells, which are small in size, found between the bases of the columnar cells. The regenerative cells are present individually or in clusters of few cells, each cell contains a large nucleus surrounded by a granular cytoplasm. The lumen of the ventriculus is surrounded by the peritrophic membrane which envelop the food-materials and protects the epithelial cells from contact with the food mass.The normal integument of larvae of *S. littoralis* (Fig. 9) consists histologically of the outer sheath of the intestine, which includes two types of muscles, the outer one is composed of one layer of longitudinal muscles, and the inner one is a layer of circular muscles.

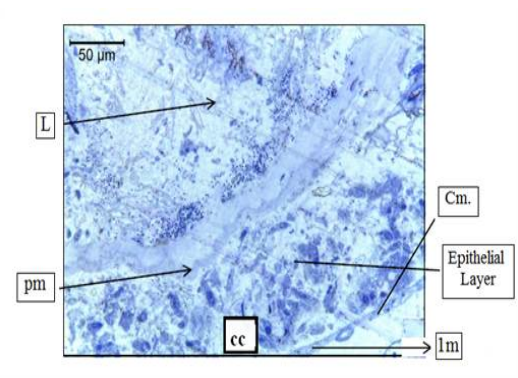

Figure 7: Cross section in the normal midgut of *S.littoralis* larval stage Im: longitudinal muscle layer; cm: circular muscle layer; cc: columnar cell; pm: peritrophic membrane; 1: lumen.

As shown in Figs. 8 and 9, treatment of 2nd instar larvae of *S. littoralis* with LC_{50} of (HP-AuNPs) nanocomposite induced remarkable histological changes in the larval midgut compared to the control samples. The epithelial cells were destroyed, vaculated, shrinked and became unclear structure. As shown in Fig. 10, the cuticle layer it's obvious that endocuticle layer was impaired and detached. Electron microscope investigation revealed obvious fissure and breaked down of (Fig. 11b) that could attributed to the destruction of the sarcolemma(Fig. 11a). As previous review the treratment of 4th instar larvae of *S. littoralis* with LC_{50} of cypermethrin according to [39]. showed swelling and separation of the hypodermal cells from the endocuticle and the hypodermal cells showed several mitotic divisions and some fissure. In the current study, certain dark spots can be observed in the larval midgut tissue which probably represent diffusion of gold nanoparticles. Treated midgut epithelial layer showed another histopathological effects. Where, epithelium got detatched from the gut wall and subsequent collapse into the gut lumen were clearly seen.

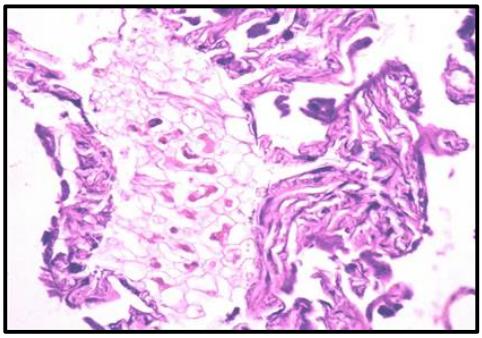

Figure 8: Cross-section in midgut larvae after treatment with LC_{50} of (HP-AuNPs) photosensitizer followed by exposure to artificial light (500 W, 4 h).

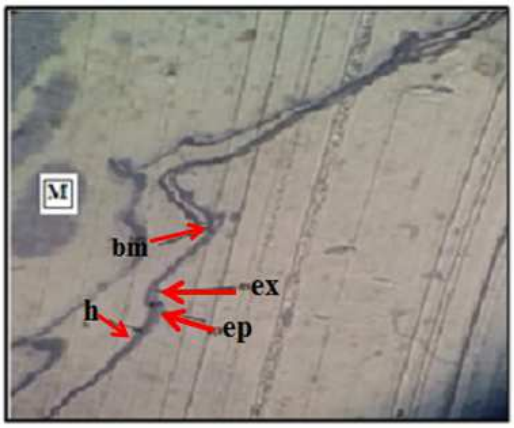

Figure 9: Cross-sectionin cuticle untreated larvae of 2nd instar En: endocuticle; ep: epicuticle; ex: exocuticle; bm: basement membrane; h: hypodermis.

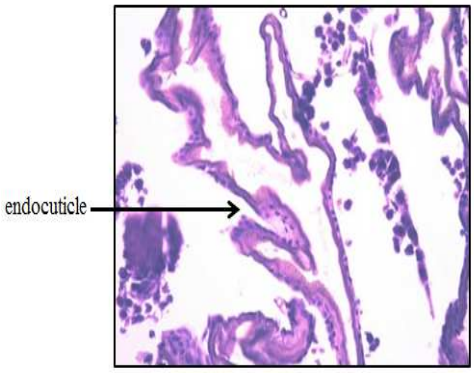

Figure 10: Cross-section in cuticle after treatment with LC_{50} of (HP-AuNPs) photosensitizer followed by exposure to artificial light (500 W, 4 h).

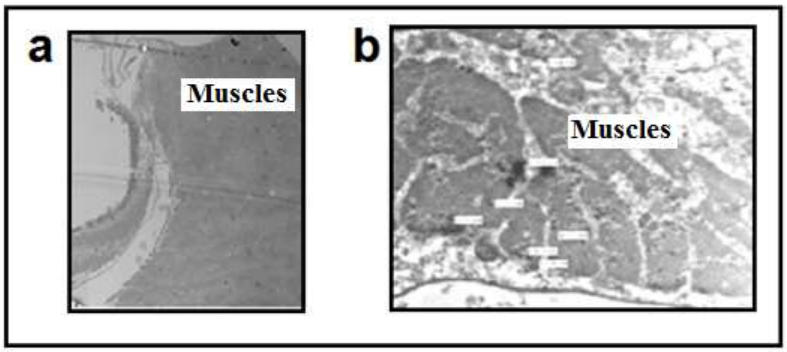

Figure 11: TEM micrographs of cross-section in cuticle larvae after treatment with LC_{50} of (HP-AuNPs) photosensitizer followed by exposure to artificial light (500 W, 4 h).

4. Conclusions

Hematoporphyrin-gold (HP-AuNPs) nanocomposite was prepared via one-pot cost-effective method. The prepared nanocomposite was characterized by TEM, FTIR, and UV-Visible spectroscopy. The photopesticidal efficiency of the prepared nanocomposite was evaluated via several techniques. The prepared nanocomposite demonstrated high photopesticidal efficacy against the second larvae instar of cotton leafworm, *S. littoralis* due to the photodynamic action of HP. The prepared photopesticide resulted in obvious disorders on the biological enzymes of *S. littoralis* and remarkably histopatathological impacts on the second larval instar of *S.littoralis*. Treatment of *S. littoralis*with the prepared nanocomposite via dipping method for 4 h followed by light exposure (halogen lamb 500 W) exhibited an obviousdisturbance of α- and β-esterase activities, alkaline phosphatase, total protein, total carbohydrate, acetyle choline esterase and mixed function oxidase activity.

5. Conflicts of interest

"There are no conflicts to declare".

6. Formatting of funding sources

No fund received.

7. Acknowledgments

We are grateful for Dr. Tarek Amin Rais for fruitful discussions.

8. References

[1]Global Cotton Outlook 2022/23- 2031/32. International Center for Agricultural Competitiveness Department of Agricultural and Applied Economics Texas Tech University.

https://www.depts.ttu.edu/aaec/icac/pubs/cotton/global-cotton-baselines/Final-Baseline-ar2022.pdf.
[2] Production and exports of Egyptian cotton increasing significantly (2017, August 30). TextileToday.Retreivedfrom https://textiletoday.com.bd/production-exports-egyptian-cotton-increasing-significantly/.
[3] Clapham, W.B. (1979). Agricultural System Structure and the Egyptian Cotton Leafworm. IIASA Working Paper. IIASA, Laxenburg, Austria: WP-79-079.
[4] Shaurub, E., El-Meguid, A., El-Aziz, A. and Nahla, M. (2014). Effect of some environmental factors on the toxicity of azadirachtin to the egyptian cotton leafworm spodoptera littoralis (Boisduval) (Lepidoptera: Noctuidae).", Ecol. Balk., 6, 113-117.
[5] Matthews, G. and Tunstall, J. (1994).Insect pests of cotton, Commonwealth Institute of Intomology.Chapter 24,p. 463.
[6]Abd El-Naby, S., (2017). Effect of chlorophyllin compound (photosensitizer) on main metabolites level of *spodoptera littoralis*, total carbohydrates,total proteins, and total lipid. *J. Biolog. Sci.* 10, 53-66.
[7]Sun, C., Cui, H., Wang, Y., Zeng, Z., Zhao, X. and Cui, B. (2016). Studies on applications of nanomaterial and nanotechnology in agriculture. *J. Agric. Sci. Technol.* 18, 18-25.
[8] Moreira, L. M., dos Santos, F. V., Lyon, J. P., Maftoum-Costa, M., Pacheco-Soares, C., and da Silva, N. S. (2008). Photodynamic therapy: porphyrins and phthalocyanines as photosensitizers. *Aus. J. Chem.* 61, 741-754.
[9]Amor, T., and Jori, G. (2000). Sunlight-activated insecticides: historical background and mechanisms of phototoxic activity. *Insect Biochem.and Mol. Biol.* 30, 915-925.
[10] Daub, M., Herrero, S., and Chung, K. (2013). Reactive oxygen species in plant pathogenesis: the role of perylenequinone photosensitizers. *Antioxid.Redox Signal.* 19, 970-989.
[11] Kalyane, D., Raval, N., Maheshwari, R., Tambe, V. and Tekade, R. K. (2019). Employment of enhanced permeability and retention effect (EPR): Nanoparticle-based precision tools for targeting of therapeutic and diagnostic agent in cancer. *Mat. Sci. Eng. C* 98, 1252-1276.
[12]Al-NoriT. (2012).Antibacterial activity of silver and gold nanoparticles against *Streptococcus*, *Staphylococcus aureus* and *E. coli*.*Al-Mustansiriyah J. Sci.* 23,45-54.
[13]Al-Sherbini, A., Khalil, M., El-Sayed, H., and Soliman, A. (2018). Prolonged preservation of corn oil via gold nanoparticles.*J. Food Process. Preserv.* 3, 1-8.
[14]El-Defrawi, M., Toppozada, A., Mansour, N., and Zeid, M. (1964). Toxicological studies on the Egyptian cotton leaf worm *Prodenia litura* L. susceptibility of different larval instar of *Prodenia* to insecticides. *J. Econ. Ent.* 57, 591-593.
[15]Abbott, W., (1925).A method of computing the effectiveness of an insecticide.*J. Econ. Etomol.* 18, 265-277.
[16]Finney, D.(1971).Probit analysis: a statistical treatment of the sigmoid response curve. A Book from Cambridge Univ., London, 333p.
[17]Simpson, D., Bulland, D.,and Linquist, D. (1964). A semi-microtechnique for the estimation of cholinesterase activity in boll weevils. *Annals of the Entomological Society of America*57, 367-371.
[18]Hansen, L., and Hodgson, E. (1971). Biochemical characteristics of insect microsomes. N-and O-demethylation. *Biochem.Pharmacol.* 20, 1569-1578.
[19]Powell.M.and Smith,M. (1954).The determination of serum acid and alkaline phosphatase activity with 4- aminoantipyrine. (AAP). *J Clin.Pathol.*7, 245-248.
[20]DuBios, M., Gilles, K., Hamilton, J., Rebers, P. and Smith, F.(1956).Colorimetric method for determination of sugars and related substances.Anal. Chem. 28, 350-356.
[21]Crompton, M. and Birt, L. (1967). Changes in the amounts of carbohydrates, phosphagen, and related compounds during the metamorphosis of the blowfly, Lucilia cuprina. *J. Insect physiol.*13, 1575-1595.
[22]Bradford, M. (1976). A rapid and sensitive method for the quantitation of microgram quantities of protein utilizing the principle of protein-dye binding. *Anal. Bio Chem.* 72, 248-254.
[23]Bozzola, J. and Russell, L. (1999). Electron Microscopy, Second Edition. Sudbury, MA: Jones and Bartlett Publishers, 670p.
[24]El-Heneidy, A., Khidr, A., and Taman, A.(2015). Side-effects of insecticides on non-target organisms: 1- in Egyptian cotton fields. *E.J.B.P.C* 25, 685-690.
[25]Ishaa Ya, I. and Klein, M. (1990). Response of susceptible laboratory and resistant field strains of *Spodoptera littoralis* (Lepidoptera: Nectuidae) to teflubenzuron. *J. Econ. Entomol.* 83, 59-62.
[26]Wu H. (2007). A study on susceptibility and biochemical mechanisms of Oxya chinensis (Thunberg) to malathion in China. Ph D thesis, Shanxi University, Shanxi Province, China. pp 87-96.
[27]Valeria De Matteis, *et. al.* (2024) Multishaped bio-gold polyphenols bearing nanoparticles to promote inflammatory suppression.Nano Today 57, 102329.
[28](a) Lei, T., Glazner, G., Duffy, M., Scherrer, L., Pendyala, S., and Huang, Z. (2012). Optical properties of hematoporphyrin monomethyl ether (HMME), a PDT photosensitizer, Photodiagn. Photodyn. Therapy, 9, 232-242. (b) Loutfy, Samah A., et al. (2013). Metallic nanomaterials as drug carriers to decrease side effects of chemotherapy (in vitro: cytotoxicity study)." J Nanopharm, Drug Deliv. 1, 1-12, 138-149.
[29]Modiano, S., and Lim, B. (1986). FT IRStudies on the active component of hematoporphyrin derivative, *Chem. Phys. Let.* 125, 333-335.
[30]Ding, L., Xu, F., Luo, B., et al. (2024). Preparation of hematoporphyrin-poly(lactic acid) nanoparticles encapsulated perfluoro-pentane/salicylic acid for enhanced US/CEST

MR bimodal imaging*Int. J Nanomed.* 19, 4589-4605.
[31]Ben Amor, T., Bortolotto, L. and Jori, G., (1998).Porphyrins and related compounds as photoactivatable insecticides. 2. phototoxic activity of meso-substituted porphyrins. *Photochem.Photobiol.* 68, 314-318.
[32]Younis, M., Hussein, A., Aboelela, H. and Rashed,G.(2021). The potential role of photosensitizers in fight against mosquitoes: phototoxicity of Rose Bengal against *Culex Pipiens* larvae. *Benha Medical Journal*, 38 (Academic issue), 1-10.
[33]Gamartificial light of halogen lamp of 500 W/m^{2}aleia, N., Shishko, E., Dolinsky, G., Shcherbakov, A., Usatenko, A. and Kholin, V. (2010). Photodynamic activity ofhematoporphyrin conjugates withgold nanoparticles: experiments in vitro. *Experimental Oncology* 32, 44-47.
[34]Abd EL-NABY, S. (2019). Toxicity of chlorophyllin compound on field and susceptible strains of *Spodopteralittoralis*, and its biochemical impact on A, B and acetylcholin-esterases. *Egy.JAgricultural Res*. 97, 89-100.
[35]Abd-El-Aziz, H. and Thabit, A. (2021).Field application and biochemical studies of certain selected photosensitizer against black cutworm,*Agrotisipsilon*. *Egy.Acad.J Biol. Sci.A, Entomology* 14, pp.47-58.
[36]Abdelsalam, S., Korayem, A., Elsherbini, E., Abdel-Aal, A., and Mohamed, D. (2014). Photosensitizing effects of hematoporphyrin dihydrochloride against the flesh fly *Parasarcophaga argyrostoma* (Diptera: Sarcophagidae). *Florida Entomologist*, 30, 1662-1670
[37]Abd El-Naby, S., and Amin, T. (2019). Impact of Chlorophyllin Dye on some Enzyme Systems of the Cotton Leafworm, *Spodoptera littoralis* (Boisd.) *Journal of Plant Protection and Pathology, Mansoura Univ*. 10, 359-362.
[38]Zaghloul, K., Hassan, E. and Abdel Kader, M.(2008). Hematoporphyrin toxicity in the cultured *Oreochromis niloticus*. *Egypt J ExpBiol (Zool)* 4, 81-88.
[39]Hassan, N., El-Metwally, H., Barakat, D., Attia, E., and Amer, R. (2016).Ultra structural deleterious in the cotton leaf worm, *Spodoptera littoralis* (Boisd.) larvae treated with certain insecticides. *J Plant Protec.Pathol.* 7, 123-136.